Giant M_2L_3 metallo-organic helicate based on phthalocyanines as a host for electroactive molecules

Ettore Fazio,[a] Cally J. E. Haynes,[b] Gema de la Torre,*[a,d] Jonathan R. Nitschke,*[b] and Tomás Torres*[a,c,d]

An unprecedented Fe_2Pc_3 metallo-organic helicate has been assembled using a bidentate phthalocyanine (Pc) ligand, 2-formylpyridine and $Fe(OTf)_2$. This giant helicate has proved itself as host for large redox-active guests such as fullerene and naphthalenediimide derivatives. Photoactivated electronic interactions between components occur in the host-guest complex.

In the last decade, important efforts have been made towards the construction of stable metallo-organic complexes through the formation of dynamic coordinative (N→metal) and covalent imine bonds in a single overall process.[1,2] Following this strategy, either edge-bridged M_4L_6 tetrahedral capsules or M_2L_3 helicates can be formed using bidentate ligands and octahedral metal centers, depending on the binding angle of the ligand.[3,4] Some of these metallo-organic ensembles provide cavities for the encapsulation of guest molecules. In particular, the construction of capsules with large defined spaces for encapsulation of large organic, electroactive guests is a stimulating challenge. In this regard, bidentate perylene bisimide,[5] and porphyrin[6] ligands have been used to build cages endowed with a very large aromatic internal surface, which are able to form stable 1:1 complexes with C_{60} fullerene. These complexes comprising photo- and redox-active host and guest components are very appealing to study electron- and energy transfer processes. In this regard, phthalocyanines (Pcs) [7] are outstanding molecules with a stronger and red-shifted absorption compared to porphyrins, and also an exceptional robustness and redox tunability, which has prompted their use as catalytic systems and as dyes for energy conversion schemes.[8–10] Worthy of mention is the extensive work reported in the literature on the excited state interactions between electron-donor Pcs and electron-acceptor species, such as fullerenes[11,12] and perylendiimides,[13] in covalent and non-covalent ensembles. Here, we describe for the first time the use of a bidentate Pc ligand for the construction of a large, optically and electronically active, metallo-supramolecular cage (i.e., Fe_2Pc_3 helicate) prepared by Fe(II)-templated subcomponent self-assembly. To the best of our knowledge, this is the first time that a Pc ligand is used to construct a metallo-organic cage, resulting in the largest M_2L_3 helicate reported to date. This ensemble is able to form 1:1 complexes with C_{60} and C_{70} fullerenes, and imidazolyl-functionalized naphthalendiimide (NDI) derivatives. In addition, the Fe_2Pc_3 host is able to trigger photoinduced charge transfer to the NDI guest, which proves this assembly as a possible container for photoactivated transformations.

The use of Pcs to self-assemble metallo-organic hosts relies on the preparation of unsymmetrically functionalized derivatives holding two opposite bridging units, which is not a trivial task and has precluded the previous use of Pcs as ligands in this area. We have recently described the regioselective preparation of soluble Pcs functionalized with iodine atoms in crosswise isoindole subunits (i.e., **1** in Scheme 1).[14,15] Importantly, the presence of iodine atoms in opposite isoindoles of the Pc offers us a unique opportunity for the preparation of ditopic ligands. It is worth mentioning that **1** comprises two regioisomers due to the relative orientations of the iodine atoms and, therefore, two Pc ligands with different coordination geometries, namely *syn* and *anti*, can be obtained and explored as building blocks for the assembly of metallo-organic structures. In fact, we have prepared Pcs **4a** (*anti*) and **4s** (*syn*), both endowed with amino groups at crosswise isoindoles (Scheme 1), for building Pc-based ensembles. Generally speaking, Pc regioisomers are very difficult to separate by chromatographic means owing to their very similar structural features. However, separation of the positional isomers was, indeed, achieved after functionalization of the starting Pc **1** with propargyl alcohol under Sonogashira conditions. The resulting mixture of Pcs **2a** and **2s** was

[a] *Departamento de Química Orgánica, Universidad Autónoma de Madrid, C/ Francisco Tomás y Valiente 7, 28049-Madrid.*
[b] *Department of Chemistry, University of Cambridge, Cambridge CB21EW, UK.*
[c] *IMDEA Nanociencia, C/Faraday, 9, Cantoblanco, 28049 Madrid, Spain.*
[d] *Institute for Advanced Research in Chemical Sciences (IAdChem), Universidad Autónoma de Madrid, 28049 Madrid, Spain.*
† Footnotes relating to the title and/or authors should appear here.
Electronic Supplementary Information (ESI) available: [details of any supplementary information available should be included here]. See DOI: 10.1039/x0xx00000x

separated by several column chromatography purification cycles (see ESI). The structural identification of the two regioisomers was obtained from ^{1}H-NMR spectroscopy (Fig. S1). For the *anti* isomer **2a**, the spectrum shows an AB system for the Pc protons of the isoindoles functionalized with bis(trifluoromethyl)phenyl units, which appear as a broad singlet at 8.28 ppm. However, the C_{2v} isomer **2s** exhibits in the spectrum two signals for the same protons at 8.27 and 8.29 ppm, which were unequivocally assigned as two singlets through a COSY experiment (Fig. S2). An ultimate proof of the correct identification of the two regioisomers arose from X-ray diffraction studies of single crystals from **2a** (Fig. S3), which confirmed the initial assignment. Finally, transformation of **2a** and **2s** in **4a** and **4s**, respectively (Scheme 1) was achieved by one-pot oxidation-decarboxylation of the propargyl groups to give **3a** and **3s**, followed by Sonogashira coupling with *p*-iodoaniline.

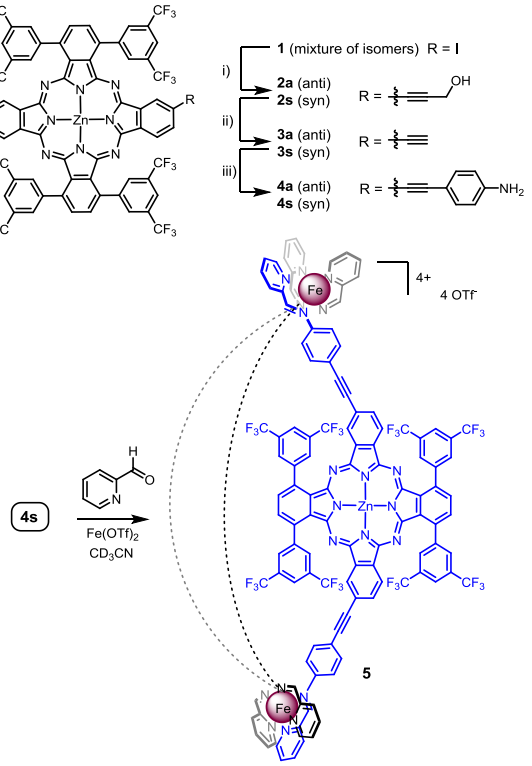

Scheme 1. Top: synthesis of Pcs **4a** and **4s**. Conditions: i) propargylic alcohol, $Pd(PPh_3)_4$, CuI, NEt_3, THF; ii) MnO_2, KOH, Et_2O; iii) *p*-iodoaniline, $Pd(PPh_3)_4$, CuI, NEt_3, THF. Bottom: Self-assembly of Pc **4s**, 2-formylpyridine and $Fe(OTf)_2$ to yield $Fe^{II}_2L_3(OTf)_4$ helical structure **5** (Fe^{II} = purple).

Next, we performed self-assembly experiments with Pcs **4a** and **4s** (Scheme 1). First, the reaction of the *syn* Pc **4s** (3 equiv) with 2-formylpyridine (6 equiv) and $Fe(OTf)_2$ (2 equiv) in CD_3CN at room temperature under nitrogen atmosphere yielded in 24h the $Fe^{II}_2Pc_3(OTf)_4$ assembly **5**, as confirmed by MS, ^{1}H-NMR, ^{19}F-NMR, DOSY, COSY and UV-vis spectroscopy (ESI, Fig. S4-S12). However, all the attempts to form metallo-supramolecular ensembles from *anti* Pc **4a** were fruitless, affording in all cases complex dynamic mixtures of coordination species.

Electrospray ionization time-of-flight (ESI-TOF) mass spectrum of **5** shows three peaks that fit with a $[Fe^{II}_2Pc_3]^{4+}$ structure (Fig. S4). The most abundant peak observed at *m/z* = 1403.9029 presents the typical *m/z* splitting for a +4 charged species, and is assigned to $[Fe^{II}_2Pc_3]^{4+}$ (Fig. 1). Two less abundant peaks appearing at *m/z* = 1921.5208 and 2956.7497 are assigned to helicate-counterion complexes $[Fe^{II}_2L_3](OTf)^{3+}$ and $[Fe^{II}_2L_3](OTf)_2^{2+}$, respectively (Fig. S5 and S6).

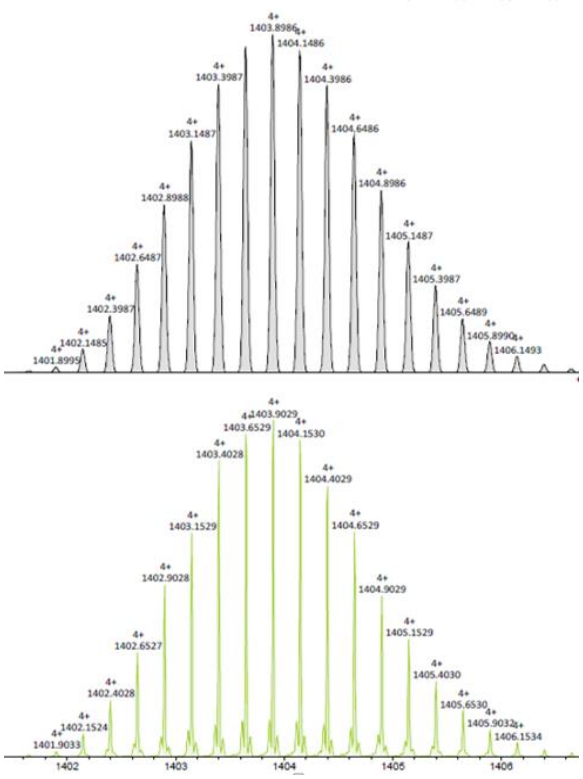

Fig. 1. High resolution ESI mass spectrum of **5**, showing the observed z = +4 charge for the peak at *m/z* = 1403.9029 (bottom) compared to the theoretical isotopic pattern (top).

According to the chirality at both six-coordinated iron centers, Fe_2L_3 structures may exhibit three stereoisomeric configurations: ΔΔ, ΛΛ, and ΔΛ, which ultimately result in two possible architectures: homochiral helicates (ΔΔ or ΛΛ) and achiral mesocates (ΔΛ).[16,17] However, considering that two oppositely chiral centers impose a distortion from the planarity of the ligands,[18] and given the rigidity of the Pc ligand and the steric demands imposed by the bulky trifluoromethylphenyl groups, we can assume that the formation of a *meso* structure is precluded in our case. The high symmetry observed in the ^{1}H-NMR of **5** (Fig. S7 and S8) clearly points out to the formation of a homochiral ensemble, since the *meso* form would present a larger number of signals due to its lower symmetry.[19]

Strong evidence of the formation of the supramolecular assembly in solution arises from DOSY measurements. The experiments were carried out in the presence of styrene (**R**) as reference compound to calculate the hydrodynamic radius (r_s) of **5** in solution (Fig. 2), according to methodologies previously reported in the literature.[6] Diffusion coefficients (*D*) are related to the effective radius of the molecular species through the Stokes–Einstein equation ($D = k_BT/6\pi\eta r_s$) and, therefore,

they can be used to determine the size of supramolecular structures. An average experimental radius of 15.7 Å was determined for **5**, which is consistent with the value of 15.9 Å derived from the model shown in Fig. 3 (see ESI and Fig. S13 for the size estimation). Moreover, the fact that the same *D* value is observed for all resonance peaks confirms the formation of a single supramolecular structure.

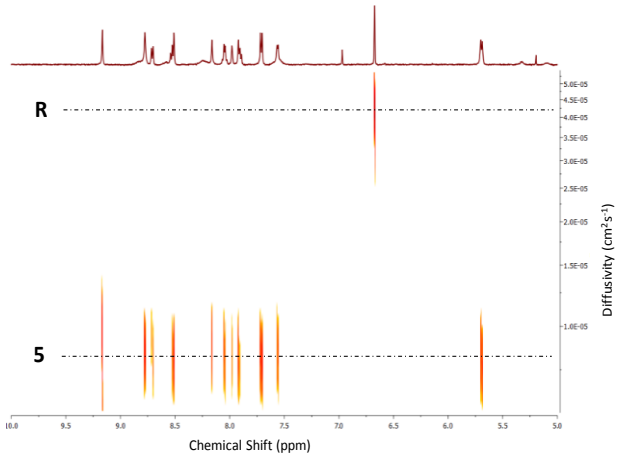

Fig. 2. Downfield portion of ^{1}H DOSY NMR spectrum of **5** in CD_3CN.

A comparison of the absorption spectra of helicate **5** and the starting Pc ligand **4s** indicates that, although Q bands from **4s** and **5** appear at the same wavelength, the extinction coefficient of **5** is much larger, as the helicate is comprised of three Pc nuclei (Fig. S12). A qualitative comparison of the fluorescence spectra of solutions of **4s** and **5** at a similar effective concentration of Pc units, shows similar emission intensities for the two species, with a slight shift to lower wavelengths of the helicate **5** with regard to the mononuclear Pc **4s**.

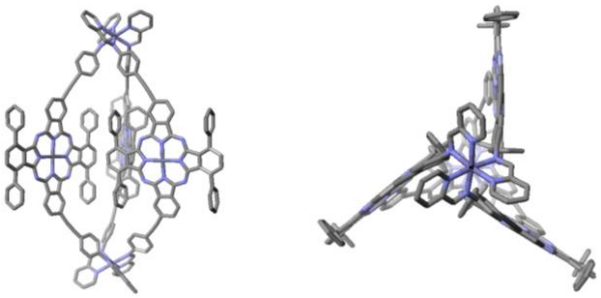

Fig. 3. a) Side view and b) top view of an energy-minimized structure of **5**, depicted with all Fe(pyridylimine)$_3$ vertices in the Λ conformation. Hydrogen atoms and trifluoromethyl groups are omitted for the sake of clarity (C = grey, N = blue, Fe = purple, Zn = dark grey).

The geometry of **5** was optimized by semiempirical calculations (PM3) starting from the ΛΛ diasteromer using the Scigress Software Suite.§ The energy-minimized structure (Fig. 3) exhibits a metal-metal distance of 27.4 Å between Fe^{II} centers, and an average separation of 13 Å between the Zn(II) ions of the Pc cores. The energy-minimized model highlights an arching of the Pc ligand in the ensemble, which seems to indicate that the Pcs in the helicate may bend to accommodate large guests. Please notice that the bent structure of the Pc units increases the effective size of the internal cavity, which was estimated to be *ca*. 705 Å^3 by using VOIDOO (Fig. S14). To the best of our knowledge, this is the largest helicate reported to date of the M_2L_3 class.

The large aromatic internal surface of **5** makes this helicate very attractive for the complexation of fullerenes species. Moreover, taking into account the well-established electron donor role of the Pc chromophores in covalent and supramolecular ensembles with fullerenes,[11,12] the complexation of fullerenes may lead to host – to – guest charge transfer complexes. Therefore, upon addition of C_{60} and C_{70} over CD_3CN solutions of the preformed helicate **5**, spectroscopical evidences of its conversion in a host–guest complex were found. First, the encapsulation of C_{60} and C_{70} fullerenes allows their solubilization in acetonitrile – otherwise extremely insoluble. The ^{1}H-NMR spectra showed, in both cases, small downfield shifts for the imine protons of **5** in the presence of the guest, (Fig. S15 and S18). In absorption experiments a small bathochromic shift of the maximum wavelength (λ_{max}) of the Pc Q band is observed from the free helicate **5** (690 nm) to the [C_{60} ⊂ **5**]$^{4+}$ and [C_{70} ⊂ **5**]$^{4+}$ complexes (695 nm) (Fig. S16 and S19, respectively). Also, mass spectrometry experiments corroborated the formation of host-guest complexes (Fig. S17 and S20). However, the presence of free host **5** was detected in both cases. Considering that the estimated internal volume of **5** is *ca.* 705Å^3, and that the volumes of C_{60} and C_{70} are 589,2 and 685,9 Å^3, respectively, the filling of the internal volume by the fullerene species exceeds the empirical 55% rule of Rebek. Nevertheless, it should be taken into account that some fullerene complexes have shown much larger occupancies.[20] Moreover, the observed complexation of fullerenes highlights the flexibility of the cage, which may adapt its cavity size as a function of the guest. Yet, the weak binding of **5** with the fullerene species prevented further studies.

In turn, we performed complexation studies with a derivative of the electron acceptor naphthalenediimide (NDI) (**6** in Fig. 4a),[21] which could also give rise to electronic interaction with the Pc components of **5**. The functionalization of the NDI with two imidazolyl rings allowed us to take advantage of the presence of the Zn(II) atoms that can coordinate strongly to N-containing ligands. Bidentate ligand **6** is capable to bind to two Zn(II) metals, thus favouring the multiple Zn(II)-ligand coordination over the single coordination bond to Fe(II) that would destroy the helicate. Moreover, bidentate coordination in the interior of the cavity would be thermodynamically favoured versus external axial binding to the Zn(II) atoms of the Pcs.

Upon addition of **6** to a solution of **5** in CD_3CN, all the components remain dissolved, which indicates that the helicate structure is preserved. ^{1}H-NMR spectrum of the solution (Fig. S21 and S22) showed upfield shifts for the protons of the Pc in comparison with those of **5**. However, the chemical shift of the imine protons do not suffer any variation upon complexation. Interestingly, we do not observe a desymmetrization of the ^{1}H-NMR signals of the complex, probably due to the dynamic nature of the binding. HR-ESI-MS experiments corroborated the

formation of a 1:1 complex with the ditopic ligand **6** (Fig. S23 and S24).

The formation of the [**6** ⊂ **5**] complex was followed by absorption and fluorescence titrations (ESI).[22] Addition of the guest **6** over solutions of **5** in CH_3CN caused both a bathochromic shift and a decrease of the intensity of the Pc-centered Q band in the absorption spectra, with the formation of a clear isosbestic point at 705 nm (Fig. 4c). Also, a strong quenching of the Pc-based emission band (λ_{exc} = 680 nm) in fluorescence spectra was observed throughout the titration (Fig. 4b). This quenching may be related to a photoinduced charge transfer from the photoexcited Pc to the electron acceptor NDI. Please note that the LUMO level of NDI lies at -4,1 , while LUMO of Pc is at -3,9 as extracted from CV experiments using Fc/Fc^+ as external reference. For both emission and absorption assays, Job's plot experiments confirmed the formation of 1:1 complexes with maxima at 0.5 molar fraction (Fig. S25). Non-linear curve fitting of the changes in absorption and fluorescence titrations allowed to determine the association constants (K_{abs} and K_{em}, respectively) for complex [**6** ⊂ **5**], using ReactLabTM EQUILIBRIA software. In this way, $logK_{abs}$ and $logK_{em}$ were respectively estimated as 5.36 ± 0.018 and 5.17 ± 0.018.

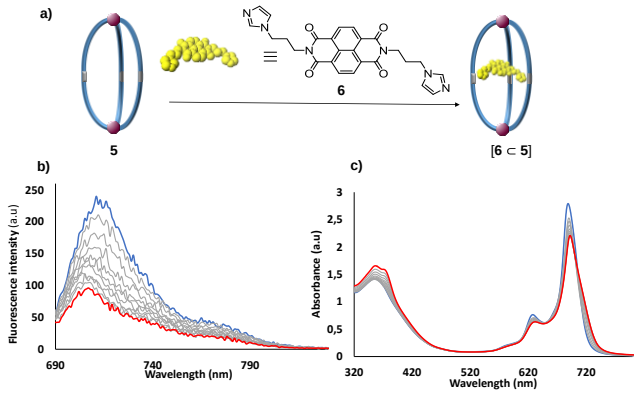

Fig 4. a) Schematic representation of the formation of host-guest complex [**6** ⊂ **5**]. b) Emission titration ($\lambda_{excitation}$ = 680 nm) and c) absorption titration of helicate **5** (10 μM) with **6**, from 0 eq. (blue lines) to 4 eq. (red lines) in CH_3CN:$CHCl_3$ 20:1 at 25 °C.

Importantly, additional control experiments were performed to establish that **5** and **6** form a host-guest complex rather than a simple imidazole-Zn(II) coordination involving only one Pc core. Thus, the addition of **6** to a solution of the mononuclear Pc **4s** did not cause any change in the Q band absorption, and a negligible quenching of the emission of the Pc molecule throughout the titration (Fig. S26), which also confirms that the excited-state interactions between the Zn(II)Pc and the NDI are enhanced in the host-guest complex.

In conclusion, we have described for the first time the use of a Zn(II)Pc as ditopic ligand for the preparation of a giant metallo-organic Fe_2Pc_3 helicate **5**, using Fe(II)-templated subcomponent self-assembly. Worth of mention is the formation of 1:1 complexes between **5** and C_{60} and C_{70} fullerenes, as detected by ^{1}H-NMR and ESI-MS experiments. Nevertheless, the most outstanding result is the formation of a very stable 1:1 complex with the bisimidazolyl-NDI derivative **6**. Experimental evidences point out to a binding of the ditopic NDI-ligand **6** to the helical host **5** through two simultaneous coordination bonds with two metallic Zn(II) located into Pc cores. Importantly, this stable host-guest complex [**6** ⊂ **5**] proved increased photoinduced interactions between the donor Pc of the helicate **5** and the acceptor NDI with regard to those exhibited my mixtures of **6** and mononuclear Zn(II)Pcs, as assessed by fluorescence titration experiments. Therefore, helicate **5** has proved its potential to form photo- and redox-functional self-assemblies.

Financial support from Comunidad de Madrid, Spain (S2013/MIT- 2841, FOTOCARBON), and Spanish MICINN (CTQ2014-52869-P) is acknowledged.

Conflicts of interest

There are no conflicts to declare

Notes and references

§ Version FJ 2.8 (EU 3.2.2), n.d.

1 M. E. Belowich, J. F. Stoddart, *Chem. Soc. Rev*. 2012, **41**, 2003.
2 S. Zarra, D. M. Wood, D. A.Roberts, J. R. Nitschke, *Chem. Soc. Rev.* 2015, **44**, 419.
3 S. E. Howson, A.Bolhuis, V. Brabec, G. J. Clarkson, J.Malina, A. Rodger, P. Scott, *Nat Chem* 2012, **4**, 31.
4 L. R. Holloway, H. H. McGarraugh, M. C. Young, W. Sontising, G. J. O. Beran, , R. J. Hooley, *Chem. Sci.* 2016, **7**, 4423.
5 K. Mahata, P. D. Frischmann, F. Würthner, *J. Am. Chem. Soc.* 2013, **135**, 15656.
6 D. M. Wood, W. Meng, T. K. Ronson, A. R. Stefankiewicz, J. K. M. Sanders, J. R. Nitschke, *Angew. Chemie Int. Ed.* 2015, **54**, 3988.
7 B. Sorokin, *Chem. Rev.* 2013, **113**, 8152.
8 M. V. Martinez-Diaz, G. de la Torre, T. Torres, *Chem. Commun.* 2010, **46**, 7090.
9 H. Imahori, T. Umeyama, K. Kurotobi, Y. Takano, *Chem. Commun.* 2012, **48**, 4032.
10 G. de la Torre, G. Bottari, T. Torres, *Adv. Energy Mater.* 2017, ***7***, 1601700.
11 G. Bottari, D. Olea, C. Gomez-Navarro, F. Zamora, J. Gómez-Herrero, T. Torres, *Angew. Chem. Int. Ed*. 2008, **47**, 2026.
12 F. D'Souza,O. Ito, *Chem. Soc. Rev.* 2012, **41**, 86.
13 J. Fernández-Ariza, R. M. Krick Calderón, M. S. Rodríguez-Morgade, D. M. Guldi, T. Torres, *J. Am. Chem. Soc.* 2016, **138**, 12963.
14 E. Fazio, J. Jaramillo-García, G. de la Torre, T. Torres, *Org. Lett.* 2014, **16**, 4706.
15 E. Fazio, J. Jaramillo-García, M. Medel, M. Urbani, M. Grätzel, M. K. Nazeerudin, G. de la Torre, T. Torres, *ChemistryOpen* 2017, **6**, 121–127.
16 C. Piguet,G. Bernardinelli, G. Hopfgartner, *Chem. Rev.* 1997, **97**, 2005.
17 M. Albrecht, *Chem. Rev.* 2001, **101**, 3457.
18 M. Meyer, B. Kersting, R. E. Powers, K. N. Raymond, *Inorg. Chem.* 1997, **36**, 5179.
19 F. Cui, S. Li, C. Jia, J. S. Mathieson, L. Cronin, X.-J. Yang, B. Wu, *Inorg. Chem.* 2012, **51**, 179.
20 T. K. Ronson, B. S. Pilgrim, J. R. Nitschke, *J. Am. Chem. Soc.* 2016, **138**, 10417.
21 F. Billeci, F. D'Anna, S. Marullo, R. Noto, *RSC Adv.* 2016, **6**, 59502.
F. J. Rizzuto, W.-Y. Wu, T. K. Ronson, J. R. Nitschke, *Angew. Chem. Int. Ed*. 2016, **55**, 7958.